

Effect of nanosized $\text{Co}_{0.5}\text{Ni}_{0.5}\text{Fe}_2\text{O}_4$ on the transport critical current density of $\text{Bi}_{1.6}\text{Pb}_{0.4}\text{Sr}_2\text{Ca}_2\text{Cu}_3\text{O}_{10}$ superconductor

M. Hafiz and R. Abd-Shukor

Citation: [AIP Conference Proceedings](#) **1614**, 30 (2014); doi: 10.1063/1.4895165

View online: <http://dx.doi.org/10.1063/1.4895165>

View Table of Contents: <http://scitation.aip.org/content/aip/proceeding/aipcp/1614?ver=pdfcov>

Published by the [AIP Publishing](#)

Articles you may be interested in

[10 to 25-fold increase in the transport superconducting critical current density of spark-plasma sintered Bi-2223 superconductors](#)

J. Appl. Phys. **117**, 043903 (2015); 10.1063/1.4906560

[Effect of strain on critical current density in grain boundaries of superconductors](#)

AIP Conf. Proc. **1558**, 932 (2013); 10.1063/1.4825653

[Effect of combined addition of nano-SiC and nano- \$\text{Ho}_2\text{O}_3\$ on the in-field critical current density of \$\text{MgB}_2\$ superconductor](#)

J. Appl. Phys. **107**, 013907 (2010); 10.1063/1.3275504

[Effect of carbon nanotube doping on critical current density of \$\text{MgB}_2\$ superconductor](#)

Appl. Phys. Lett. **83**, 4996 (2003); 10.1063/1.1634378

[Transport critical current densities of partially aligned bulk samples of \$\text{YBa}_2\text{Cu}_3\text{O}_{7-x}\$ superconductors](#)

J. Appl. Phys. **68**, 4178 (1990); 10.1063/1.346232

Effect of Nanosized $\text{Co}_{0.5}\text{Ni}_{0.5}\text{Fe}_2\text{O}_4$ on the Transport Critical Current Density of $\text{Bi}_{1.6}\text{Pb}_{0.4}\text{Sr}_2\text{Ca}_2\text{Cu}_3\text{O}_{10}$ Superconductor

M. Hafiz and R. Abd-Shukor

*School of Applied Physics, Faculty of Science and Technology, Universiti Kebangsaan Malaysia,
43600 Bangi, Selangor, Malaysia*

Abstract. The effects of nano-sized $\text{Co}_{0.5}\text{Ni}_{0.5}\text{Fe}_2\text{O}_4$ addition on the superconducting and transport properties of $\text{Bi}_{1.6}\text{Pb}_{0.4}\text{Sr}_2\text{Ca}_2\text{Cu}_3\text{O}_{10}$ (Bi-2223) in bulk form has been investigated. Bi-2223 superconductor was fabricated using co-precipitation method and 0.01 – 0.05 wt% of $\text{Co}_{0.5}\text{Ni}_{0.5}\text{Fe}_2\text{O}_4$ nanoparticles with average size of 20 nm were added into the samples. The critical temperature (T_c) and critical current density (J_c) of the samples were measured by using the four-point probe method, while the phase formation and microstructure of the samples were examined using x-ray diffraction and SEM respectively. It was found that J_c of all samples added with $\text{Co}_{0.5}\text{Ni}_{0.5}\text{Fe}_2\text{O}_4$ were higher than non-added sample, with $x = 0.01$ wt. % sample showing the highest J_c . This study showed that small addition of nano- $\text{Co}_{0.5}\text{Ni}_{0.5}\text{Fe}_2\text{O}_4$ can effectively enhance the transport critical current density in Bi-2223 superconductor.

Keywords: Bi-2223 Superconductor, Critical Current Density, Nanoparticles.

PACS: 74.25.F-, 74.72-h, 81.07.Wx

INTRODUCTION

The $\text{Bi}_{1.6}\text{Pb}_{0.4}\text{Sr}_2\text{Ca}_2\text{Cu}_3\text{O}_{10}$ (Bi-2223) high temperature superconductor have shown great promise for commercialization to be used in various applications due to its potential of carrying high current [1-2]. However, the weak pinning force of flux lines suppresses the transport current density in applied magnetic fields and high temperature. Many studies have been made to enhance the electrical transport capabilities of Bi-2223 such as introducing nanosized particles into the superconductor to act as flux pinning centers [3-6]. Furthermore, magnetic impurities such as NiFe_2O_4 and Fe_3O_4 addition have also showed improvements in the transport properties of Bi-2223 [7-8].

Two important characteristic lengths in superconductor are the coherence length, ξ and penetration depth λ . A strong interaction between flux line network and the system can be expected if $\xi < L < \lambda$ where L is the average nanoparticle size [9]. Addition of the nanoparticles within this size range will increase the critical current density [10]. In this work, the phase formation, microstructure, transition temperature and electrical transport properties of Bi-2223 with magnetic $\text{Co}_{0.5}\text{Ni}_{0.5}\text{Fe}_2\text{O}_4$ nanoparticles addition were studied. The average size of nanoparticles employed in this study was chosen to be within the range of $\xi < L < \lambda$.

EXPERIMENTAL DETAILS

Bi-2223 superconductor powders were synthesized by conventional acetate co-precipitation method using metal acetates of bismuth, lead, strontium, calcium and copper (purity 99.99%) [11]. The dried-up powders were heated for first calcination at 730°C for 12 hours followed by a second calcination at 845°C for 24 hours. 0.01 wt% to 0.05 wt% of commercially available $\text{Co}_{0.5}\text{Ni}_{0.5}\text{Fe}_2\text{O}_4$ nanoparticles (Inframat Advanced Materials, 99.9% purity) with average size of 20 nm was added to the powders. The powders were ground thoroughly and then pressed into pellets of 13mm diameter and 2mm thickness. The pellets were sintered at 850°C for 48 hours.

The average size of $\text{Co}_{0.5}\text{Ni}_{0.5}\text{Fe}_2\text{O}_4$ was examined using a Philips CM12 transmission electron microscope (TEM). The XRD patterns of the sample were recorded using a Bruker D8 Advance diffractometer with $\text{CuK}\alpha$ radiation while the microstructures of the sample were observed by Philips XL 30 scanning electron microscope (SEM). The distribution of nano $\text{Co}_{0.5}\text{Ni}_{0.5}\text{Fe}_2\text{O}_4$ in the sample was determined by Philips PV99 energy dispersed x-ray analyzer (EDX). The electrical resistance versus temperature measurements was carried out by the four-point

probe method in conjunction with a CTI cryogenics closed-cycle refrigerator (Model 22). The pellets were then cut into bar-shapes for critical current measurements. The four-point probe method with 1 $\mu\text{V}/\text{cm}$ criterion was used to measure J_c between 30 K and 77 K.

RESULTS AND DISCUSSION

As shown in FIGURE 1, the average size of $\text{Co}_{0.5}\text{Ni}_{0.5}\text{Fe}_2\text{O}_4$ nanoparticles employed in this study was determined to be around 20 nm. The particle size is larger than the coherence length, ξ and smaller than the penetration depth, λ of Bi-2223 ($\xi = 2.9$ nm, $\lambda = 60 - 1000$ nm for Bi-2223) [12].

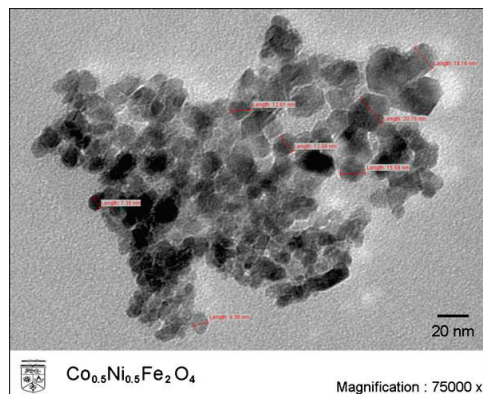


FIGURE 1. TEM image of nano $\text{Co}_{0.5}\text{Ni}_{0.5}\text{Fe}_2\text{O}_4$ used in this study.

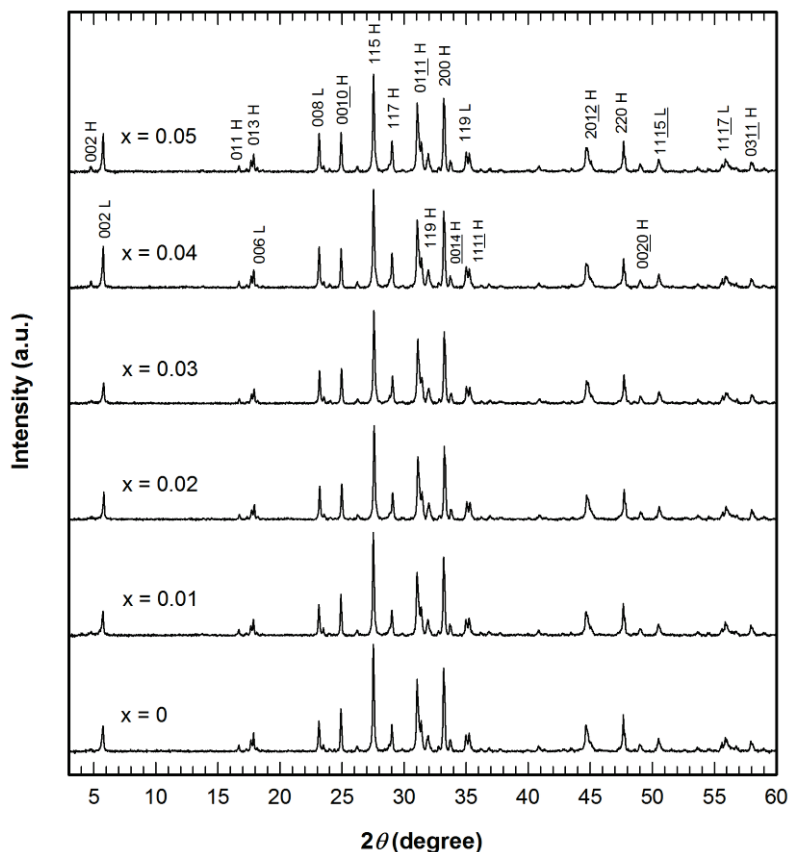


FIGURE 2. XRD patterns of the non-added and nano $\text{Co}_{0.5}\text{Ni}_{0.5}\text{Fe}_2\text{O}_4$ added Bi-2223 samples with corresponding Miller indices of each peaks. “H” denotes Bi-2223 phase and “L” denotes Bi-2212 phase.

The XRD patterns of all samples with the Miller indices are shown in FIGURE 2. The dominant XRD peaks mainly correspond to the Bi-2223 phase, labeled with “H” in the figure. A small amount of low- T_c phase (Bi-2212) peaks are labeled with “L”. Volume fraction of Bi-2223 and Bi-2212 was determined from the total intensities of both phases [13] and summarized in TABLE (1). The volume fraction of Bi-2223 increased slightly when 0.01 wt% nano $\text{Co}_{0.5}\text{Ni}_{0.5}\text{Fe}_2\text{O}_4$ was added to the sample and decreased when the addition was increased to 0.05 wt%.

The lattice parameters of the non-added sample were $a = b = 5.405 \text{ \AA}$ and $c = 37.276 \text{ \AA}$. All of the nano $\text{Co}_{0.5}\text{Ni}_{0.5}\text{Fe}_2\text{O}_4$ added samples showed similar lattice parameters, indicating that small addition of $\text{Co}_{0.5}\text{Ni}_{0.5}\text{Fe}_2\text{O}_4$ does not show significant change in the lattice parameters.

FIGURE 3 (a) and (b) show SEM the micrographs of the non-added sample and sample with 0.01 wt.% nano $\text{Co}_{0.5}\text{Ni}_{0.5}\text{Fe}_2\text{O}_4$ respectively. Both samples showed large plate-like layered microstructure which is the typical grain structure of Bi-2223. The grain morphology of all the samples are similar to each other except for minor variations in texture and porosity. The white dots in FIGURE 3 (b) show the distribution of $\text{Co}_{0.5}\text{Ni}_{0.5}\text{Fe}_2\text{O}_4$ in the sample as observed by EDX.

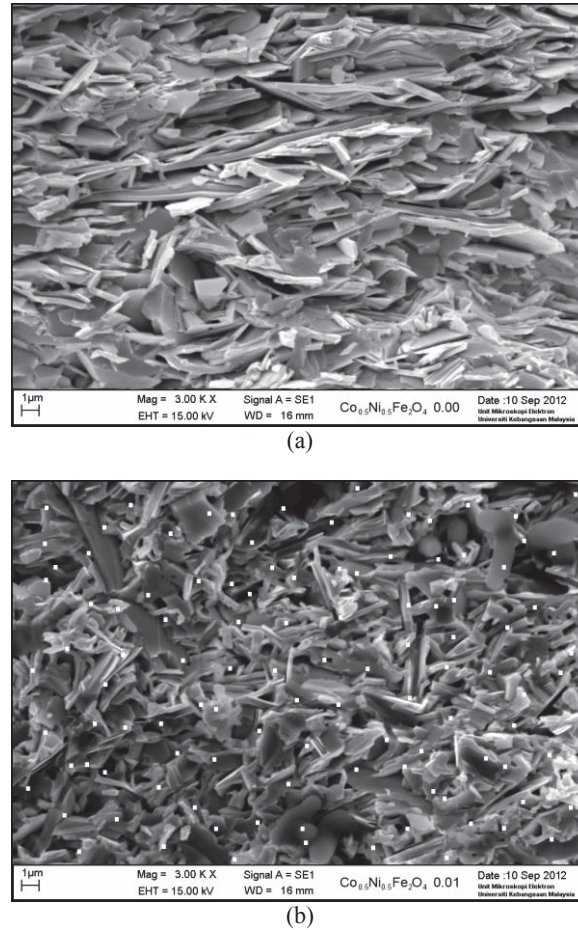


FIGURE 3. SEM micrographs of (a) non-added sample and (b) 0.01 wt.% $\text{Co}_{0.5}\text{Ni}_{0.5}\text{Fe}_2\text{O}_4$ added sample. White dots indicate the distribution of $\text{Co}_{0.5}\text{Ni}_{0.5}\text{Fe}_2\text{O}_4$ nanoparticles as observed by EDX.

FIGURE 4 shows the curve of the electrical resistance versus temperature for all the samples. All the samples showed a metallic behavior above the transition temperature. The zero resistance temperature ($T_{c \text{ zero}}$) is shown in TABLE (1). The non-added sample showed $T_{c \text{ zero}}$ at 101 K. The sample with 0.01 wt% nano $\text{Co}_{0.5}\text{Ni}_{0.5}\text{Fe}_2\text{O}_4$ showed a slightly higher $T_{c \text{ zero}}$ than the non-added sample at 102 K, while the sample with higher addition of $\text{Co}_{0.5}\text{Ni}_{0.5}\text{Fe}_2\text{O}_4$

showed a significant decrease in $T_{c\text{ zero}}$. The increased $T_{c\text{ zero}}$ in 0.01 wt% sample can be attributed to an enhancement of the high- T_c phase.

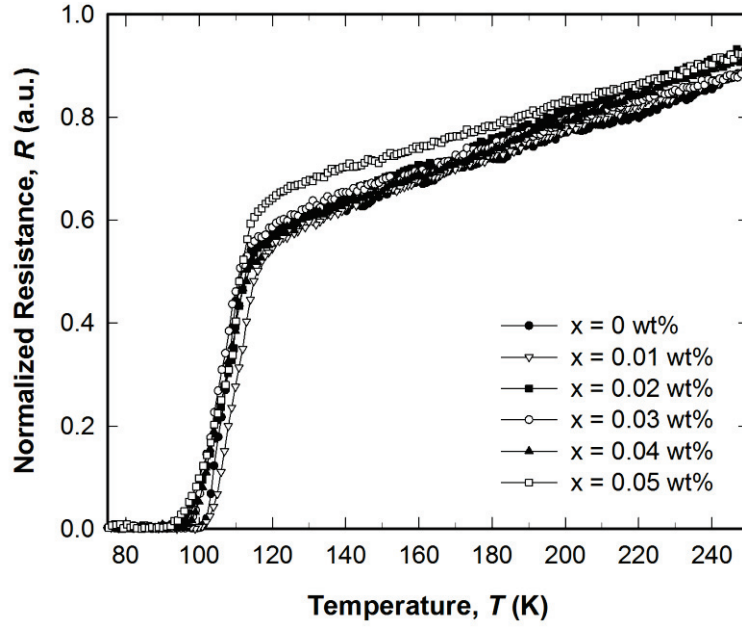


FIGURE 4. Electrical Resistance versus temperature for non-added and nano $\text{Co}_{0.5}\text{Ni}_{0.5}\text{Fe}_2\text{O}_4$ added Bi-2223 samples.

The critical current density, J_c as a function of temperature for all samples between 30 K and 77 K are shown in FIGURE 5 (a). All samples with addition of nanosized $\text{Co}_{0.5}\text{Ni}_{0.5}\text{Fe}_2\text{O}_4$ showed a higher J_c compared to non-added sample, and the J_c showed degradation with increasing temperature as a consequence of thermally activated flux creep. The highest value of J_c recorded was observed in the $x = 0.01$ wt.% sample which is 2051 mA/cm^2 at 30 K. FIGURE 5 (b) also showed that further addition of $\text{Co}_{0.5}\text{Ni}_{0.5}\text{Fe}_2\text{O}_4$ also lead to a degradation in J_c . From the J_c results, it showed that 0.01 wt.% of $\text{Co}_{0.5}\text{Ni}_{0.5}\text{Fe}_2\text{O}_4$ nanoparticles in Bi-2223 system is the optimum amount to achieving highest J_c . Previous studies with similar nanoparticles, Fe_3O_4 and NiFe_2O_4 also showed that an addition of $x = 0.01\%$ nanoparticles significantly increased the J_c of Bi-2223 superconductors [7-8].

The enhancement is believed due to the $\text{Co}_{0.5}\text{Ni}_{0.5}\text{Fe}_2\text{O}_4$ nanoparticles addition improving intergrain connectivity in Bi-2223. The nanoparticles may reside at the grain boundary or go into the grains, which play a role as effective pinning centers and leads to an increase in J_c [14].

TABLE (1). Volume fraction of Bi-2223 and Bi-2212 phase, zero resistance temperature ($T_{c\text{ zero}}$) and critical current density (J_c) at 30 K and 77 K in self field of non-added and nano- $\text{Co}_{0.5}\text{Ni}_{0.5}\text{Fe}_2\text{O}_4$ added samples.

| x (wt.%) | Bi-2223 (%) | Bi-2212 (%) | $T_{c\text{ zero}}$ (K) | J_c at 30 K (mA/cm ²) | J_c at 77 K (mA/cm ²) |
|---------------|----------------|----------------|----------------------------|--|--|
| 0.00 | 84 | 16 | 101 | 229 | 30 |
| 0.01 | 86 | 14 | 102 | 2051 | 894 |
| 0.02 | 83 | 17 | 96 | 1804 | 674 |
| 0.03 | 82 | 18 | 97 | 1182 | 333 |
| 0.04 | 83 | 17 | 97 | 1274 | 489 |
| 0.05 | 84 | 16 | 95 | 928 | 222 |

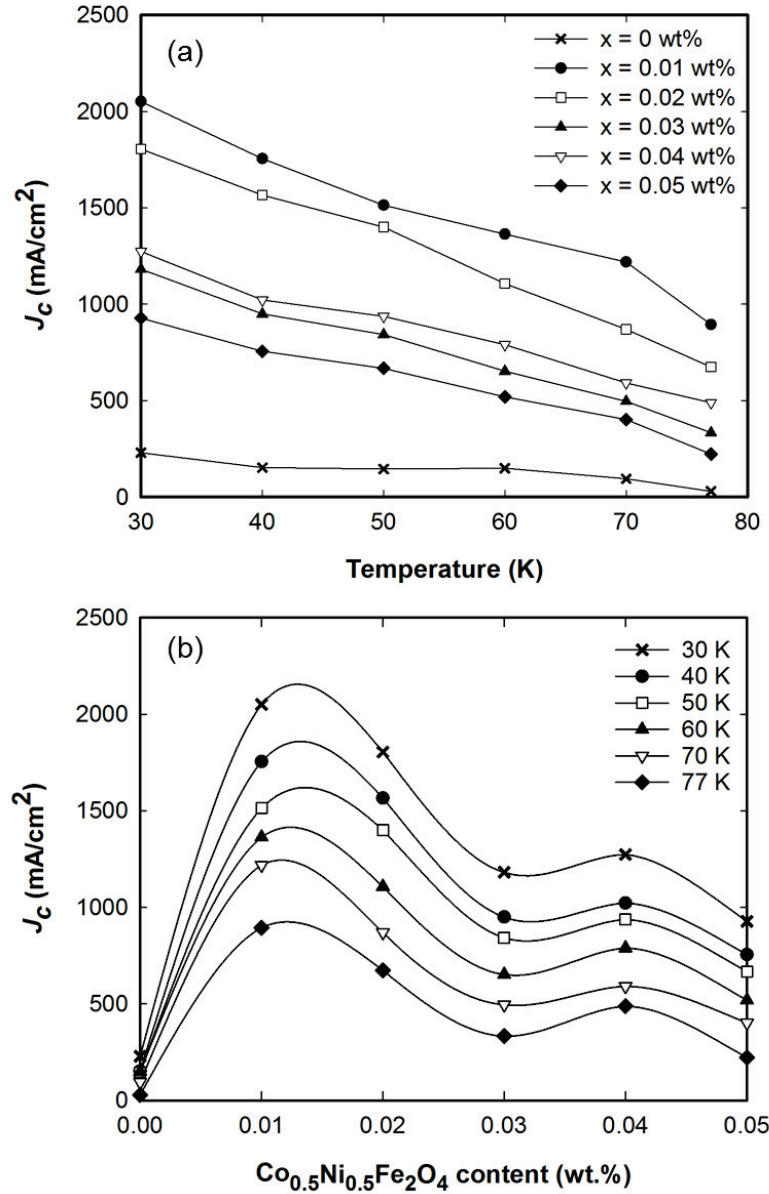


FIGURE 5. Critical current density J_c of all samples (a) as a function of temperature, and (b) content of nano $\text{Co}_{0.5}\text{Ni}_{0.5}\text{Fe}_2\text{O}_4$ between 30 and 77 K (solid lines are for eye guide).

CONCLUSION

Bi-2223 superconductor was prepared by acetate co-precipitation method. The effect nano $\text{Co}_{0.5}\text{Ni}_{0.5}\text{Fe}_2\text{O}_4$ addition on the phase formation, microstructure, and electrical transport properties on the prepared Bi-2223 has been investigated. The J_c of pellets with $\text{Co}_{0.5}\text{Ni}_{0.5}\text{Fe}_2\text{O}_4$ addition showed a significant increase compared to the non-added sample. The highest J_c and volume fraction of Bi-2223 was observed in the sample with 0.01 wt.% addition.

ACKNOWLEDGMENTS

This research was supported by the Ministry of Science of High Education under grant no. ERGS/1/2011/STG/UKM/01/25 and Universiti Kebangsaan Malaysia under grant no. UKM-DLP-2011-018.

REFERENCES

1. H. Abbasi, J. Taghipour, H. Sedghi, *Journal of alloys and Compounds* **494**, 305-308 (2010).
2. S. E. Mousavi Ghahfarokhi, M. Zargar Shoushtari, *Physica B: Condensed Matter* **405**, 4643-4649 (2010).
3. A. Ghattas, M. Annabi, M. Zouaoui, F. Ben Azzouz and M. Ben Salem, *Physica C:Superconductivity* **468**, 31-38 (2008).
4. M. Annabi, A. M'chirgui, F. Ben Azzouz, M. Zouaoui and M. Ben Salem, *Physica C:Superconductivity* **405**, 25-33 (2004).
5. Z. Y. Jia, H. Tang, Z. Q. Yang, Y. T. Xing, Y. Z. Wang, and G. W. Qiao, *Physica C:Superconductivity* **337**, 130-132 (2000).
6. I. H. Gul, F. Amin, A. Z. Abbasi, M. Anis-ur-Rehman, and A. Maqsood, *Physica C:Superconductivity* **449**, 139-147 (2006).
7. W. Kong and R. Abd-Shukor, *Journal of Superconductivity and Novel Magnetism* **23**, 257-263 (2010).
8. R. Abd-Shukor and W. Kong, *Journal of Applied Physics* **105**, 07E311 (2009).
9. U. Al Khawaja, M. Benkraouda, I. M. Obaidat and S. Alneaimi, *Physica C:Superconductivity* **442**, 1-8 (2006).
10. I. F. Lyuksyutov and D. G. Naugle, *Modern Physics Letters B* **13**, 491-497 (1999).
11. M. Ismail, R. Abd-Shukor, I. Hamadneh, and S. A. Halim, *Journal of Materials Science* **39**, 3517-3519 (2004).
12. H. L. Anderson (ed.), *A Physicist's Desk Reference* 2nd edition, New York: American Institute of Physics, 1989, pp. 118.
13. I. Van Driessche, A. Buekenhoudt, K. Konstantinov, E. Bruneel, and S. Hoste, *Applied Superconductivity* **4**, 185-190 (1996).
14. W. Kong and R. Abd-Shukor, *Journal of Electronic Materials* **36**, 1648-1651 (2007).